Dielectric properties of polar-phthalocyanine monolayer systems with repulsive dipole interaction

H. Fukagawa,[1,*] S. Hosoumi,[1] H. Yamane,[2] S. Kera,[1,†] and N. Ueno[1]

[1]*Graduate School of Advanced Integration Science, Chiba University, 1-33 Yayoicho, Inage-ku, Chiba 263-8522, Japan*

[2]*Institute for Molecular Science, Myodaiji, Okazaki 444-8585, Japan*

(Received 22 October 2010; revised manuscript received 7 January 2011; published 22 February 2011)

Changes in the work function (WF) of phthalocyanine-graphite systems were investigated as functions of phthalocyanine coverage and the value of the molecular dipole moment by using ultraviolet photoelectron spectroscopy. The dipoles in the film were found to be perpendicular to the graphite surface, and the coverage dependence of the WF of each dipole-phthalocyanine–graphite system clearly exhibited a sudden increase before the monolayer formation depending on the value of the dipole moment. The results show that the dipole-dipole repulsive interaction impacts the growth and structure of monolayer systems with weak intermolecular and molecule-substrate electronic coupling. The electric dipole moment and polarizability of each phthalocyanine in a monolayer was estimated by analyzing the observed coverage dependence of the WF using the Topping model (nanoscale method). Furthermore, it was demonstrated that the dielectric constant obtained with the nanoscale method and that estimated using the Helmholtz equation (macroscopic method) were almost the same. This agreement substantiates the application of the macroscopic model to an organic monolayer that is not a continuum medium.

DOI: 10.1103/PhysRevB.83.085304 PACS number(s): 73.30.+y, 79.60.Dp, 73.20.−r

I. INTRODUCTION

Surface dipole modifications have been of great interest for controlling surface and/or interface properties in organic and molecular electronic devices, and they are important especially in tuning the energy-level alignment at organic-metal interfaces.[1–3] Methods of controlling surface properties, particularly using self-assembled monolayers (SAMs) with the chemical moiety of an electric dipole, have been widely investigated to enhance the charge transport properties in molecule-based devices.[4–9] The electric dipole moment (P) and the dielectric constant (ε) of ultrathin organic layers are thus important parameters for discussing the electrical properties of such dipole layer systems. In the past, the work function (WF) or surface-potential change related to interface dipoles in SAMs has been analyzed using the Helmholtz equation, which is derived for continuum media.[9–11] In these analyses, therefore, a specimen is assumed to be a continuum medium. Furthermore, the effect of the dipole-dipole interaction, such as a depolarization effect and change in the total interaction energy of the film, has not been positively considered until recently, although the dipole-dipole interaction is a key factor in discussing molecular dipole systems with weak intermolecular electronic coupling.[1]

Topping proposed a depolarization model based on the calculations for a planar sheet of evenly spaced dipoles on either a square or hexagonal lattice.[12] MacDonald and Barlow addressed polarizable dipoles and suggested a form for the effective dielectric constant according to the Topping model;[13,14] this was elaborated on by Taylor and Bayes.[15] In this form, the P and polarizability (α) of a surface-molecule complex can be determined from the coverage dependence of WF in the limit of zero coverage.[16] The Topping model is an alternative to the analysis method using the Helmholtz equation and has been widely used in analyzing the change in WF by many groups, mainly for inorganic systems.[14–18] The use of the Topping model in studying modification of organic-device interfaces with polar molecules has been very limited, because it is not easy to identify molecular orientation and monolayer formation for evaporated thin films of large organic molecules. Estimation of the P, α, and ε of such organic dipole layer systems with the Topping model is required to understand more deeply the energy-level alignment at dipole-layer interfaces in organic devices.[19] Moreover, comparison of the ε values estimated using the macroscopic Helmholtz equation and nanoscopic Topping model for the same dipole system is necessary to bridge the macroscopic and nanoscale methods.[20]

For inorganic systems, MacDonald and Barlow have already clarified the connection between the Topping model and Helmholtz equation.[13] For organic systems, Natan *et al.* recently investigated this subject computationally using density functional theory (DFT) calculations.[3,21] We recently succeeded in applying this model to an analysis of the change in the WF of a vacuum-deposited well-defined dipole layer system that consists of a large π-conjugated molecule with an electric dipole moment and an inert substrate surface.[20] We estimated the P and α of OTi-phthalocyanine (OTiPc) experimentally.[20] So far, however, to the best of our knowledge, no experimental study has been performed on the impact of the dipole-dipole interaction on the structure and dielectric properties of an organic film with an electric dipole, and on bridging the macroscopic and nanoscopic methods. Understanding impacts of the dipole-dipole interaction in weakly interacting molecular systems is a key to unraveling the growth mechanism of functional organic thin films and their electronic functions both in the films and at molecule-substrate interfaces. To go deeper into these issues, we have studied dielectric properties of organic monolayer systems using polarized Pc-graphite systems as a function of the molecular dipole moments.

In the present study, ultraviolet photoelectron spectroscopy (UPS) measurements were performed on thin films of two polar phthalocyanine molecules with different electric dipole moments, OV-phthalocyanine (OVPc) and ClAl-phthalocyanine

(ClAlPc),[22,23] and nonpolar Cu-phthalocyanine (CuPc) on graphite. We studied the WF change during monolayer growth for these systems as functions of the coverage and the dipole moment of the molecule, and compared these results with that for OTiPc-graphite.[20] We observed a steplike increase in the coverage dependence of the WF before monolayer formation depending on the molecular dipole moment, resulting in a larger molecular (dipole) density and a smaller α in the monolayer than those extrapolated from a lower coverage region. By analyzing the observed WF shift using the Topping model, we estimated the P and α of the molecules in the monolayer by taking the effect of the dipole-dipole repulsive interaction into account. Furthermore, we show that the macroscopic method can offer ε similar to those obtained with the nanoscopic method, which is consistent with the recent theoretical results.[1]

II. EXPERIMENT

He I UPS spectra were measured using a previously described apparatus.[24] The total instrumental energy resolution of the present measurements was less than 60 meV as measured from the Fermi edge of an evaporated Au film. The sample was biased by −5.0 V so that the secondary electron cutoff of the spectrum would yield the vacuum level (VL). The energy difference between the VL and the Fermi level corresponds to the WF of the sample. A highly oriented pyrolytic graphite (HOPG)–ZYA-grade substrate was cleaved in air immediately before being loaded into a sample preparation chamber ($\sim 10^{-8}$ Pa) and then cleaned in the usual way by *in situ* heating at 620 K for 15 h. The purified OVPc, ClAlPc, and CuPc were evaporated onto the HOPG substrate in the sample preparation chamber at a substrate temperature of 295 K. The amount and rate (0.05 nm/min) of deposition were measured with a quartz microbalance. The sample was then introduced into the measurement chamber for *in situ* measurements. We repeatedly conducted deposition, sample annealing, and UPS measurements. All UPS spectra were measured at 295 K after annealing the films at 420 K for 3 h in order to obtain well-oriented films of monolayer and subsequent multilayers with *p*-polarized He I radiation. The angle between the incident photons and detected photoelectrons was fixed to 45° with an acceptance angle of ±12°. For all spectra, the binding energy (E_B) refers to the Fermi level of the substrate (E_F^{sub}).

III. RESULTS AND DISCUSSION

Prior to showing the experimental results, we briefly summarize here previous results of the growth of OVPc and ClAlPc thin films on HOPG, namely, the change in molecular orientation with increasing film thickness and the effect of annealing on molecular orientation.[22,23] In as-grown film on HOPG with a monolayer and a submonolayer of nominal thickness, molecules form bilayer islands in which most of the molecules in the outer layer are oriented flat with the oxygen or chlorine atom directed inward to the substrate (*downward orientation*). Upon annealing, the molecules spread from the islands over the substrate surface to form monolayer domains in which all the molecules are oriented flat, with the oxygen or chlorine atom directed outward to the vacuum (*upward orientation*). When the second layer is deposited on this monolayer, the molecules in the outer layer exhibit a *downward orientation* as in the OTiPc-HOPG system.[20,25,26] In the oriented monolayer, the electric dipole moments of the molecules are parallel with the *downward* orientation and form a two-dimensional dipole layer, whereas in the bilayer the electric dipole moments of the first and second layers cancel each other out. These changes in molecular orientation were detected by metastable atom electron spectroscopy (MAES), and the corresponding WF shift and fine structures of the highest occupied molecular orbital (HOMO) band were observed using UPS.[22,23] Such molecular orientation in the monolayer and bilayer has been recently confirmed for ClAlPc by Huang *et al.* using scanning tunneling microscopy (STM).[27]

Examples of the He I UPS spectra of OVPc, ClAlPc, and CuPc on HOPG are shown as functions of the deposition amount (δ) in Figs. 1–3, respectively. In each figure, the VL region (a) and the HOMO band region (b) are shown. The spectra of the VL region were measured at an electron takeoff angle of 0° (normal emission) and a photon incidence angle of 45°. The spectra of the HOMO band region were measured at an electron takeoff angle of 45° and a photon incidence angle of 0° (normal incidence). As seen in Fig. 1(a), the VL of the OVPc-HOPG first increases for $0 \leqslant \delta \leqslant 0.28$ nm with δ, then decreases for $0.28 \leqslant \delta \leqslant 0.66$ nm. and remains unchanged for $\delta \leqslant 0.66$ nm. In Fig. 1(b), in contrast, the HOMO band shows small changes in position and shape for $0 \leqslant \delta \leqslant 0.28$ nm and broadens with δ until $\delta = 0.56$ nm. Finally, the intensity of the higher-E_B component increases for $\delta \geqslant 0.66$. The fine

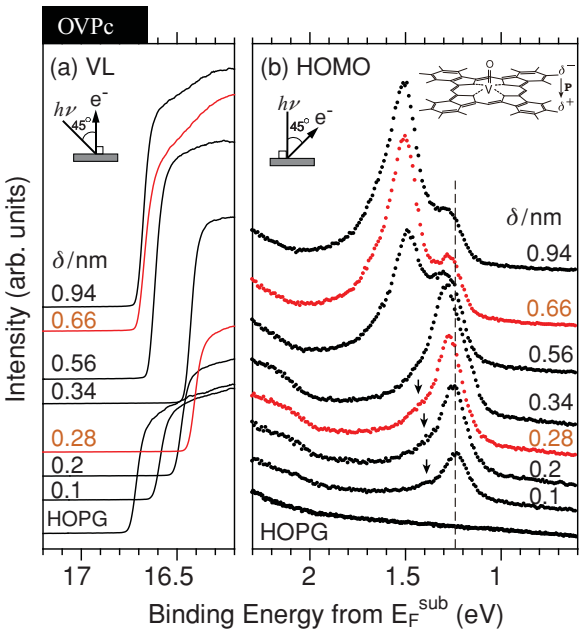

FIG. 1. (Color online) Examples of He I UPS spectra as functions of deposition amount of OVPc (δ) on HOPG (a) in the VL region and (b) in the HOMO band region. All spectra were measured at 295 K after annealing each film at 420 K for 3 h with a −5 V bias applied to the sample to observe VL. The inset shows schematics of the direction of the molecular electric dipole moment (P) and the molecular structure of OVPc.

structures in the very sharp HOMO band for $\delta \leqslant 0.28$ nm (indicated by the arrows) originate from vibration coupling of the hole and indicate that the molecules are well ordered and have an upward orientation.[22,28,29] These δ dependences of the VL and HOMO band positions exhibit the same trend observed for the OTiPc-HOPG system.[20] We also see in Fig. 1(a) that the VL increases continuously with δ up to $\delta = 0.28$ nm at ~0.3 eV. It then decreases, reaching a constant value, which is approximately similar to that of HOPG, at $\delta = 0.66$ nm. By considering the molecular orientation and the electrostatic potential owing to the permanent dipole of OVPc,[22] these results indicate that (i) the monolayer of OVPc is formed at $\delta = 0.28$ nm and (ii) the bilayer formation starts at $\delta = 0.28$ nm and is completed at $\delta = 0.66$ nm, where the dipoles in the first layer are cancelled by those in the second layer.

For ClAlPc in Fig. 2(a), the VL first increases for $0 \leqslant \delta \leqslant 0.36$ nm with δ, then decreases for $0{,}36 \leqslant \delta \leqslant 0.7$ nm, and remains unchanged for $\delta \geqslant 0.7$ nm. In Fig. 2(b), in contrast, the HOMO band shows small changes in position and shape for $0 \leqslant \delta \leqslant 0.36$ nm and broadens with δ until $\delta = 0.6$ nm. Finally, the intensity of the higher-E_B component increases for $\delta \geqslant 0.7$ nm. The fine structures in the very sharp HOMO band for $\delta \leqslant 0.36$ nm come from the vibration coupling and indicate that the film quality is very high and the molecules have an upward orientation as in the OVPc films.[22,28,29] These δ dependences of the VL and HOMO band positions are basically similar to those observed for OVPc-HOPG and OTiPc-HOPG[20] systems.

Figure 3 displays the results for the CuPc-HOPG system. The nominal deposition amount for the monolayer was 0.37 nm

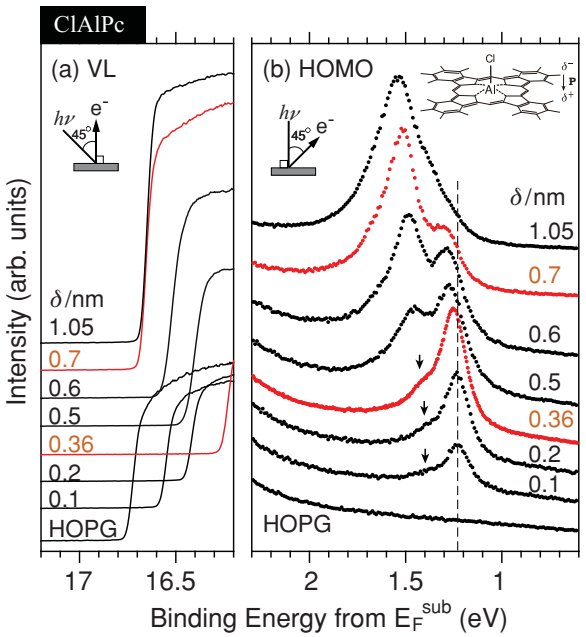

FIG. 2. (Color online) Examples of He I UPS spectra as functions of deposition amount of ClAlPc (δ) on HOPG (a) in the VL region and (b) in the HOMO band region. All spectra were measured at 295 K after annealing each film at 420 K for 3 h with a −5 V bias applied to the sample to observe VL. The inset shows schematics of the direction of the molecular electric dipole moment (P) and the molecular structure of ClAlPc.

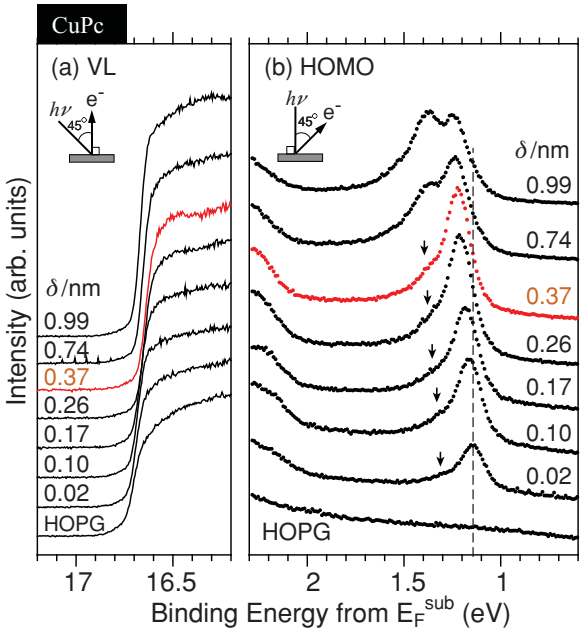

FIG. 3. (Color online) Examples of He I UPS spectra as functions of deposition amount of CuPc (δ) on HOPG (a) in the VL region and (b) in the HOMO band region. All spectra were measured at 295 K after annealing each film at 420 K for 3 h with a −5 V bias applied to the sample to observe VL.

in our experiments, which was determined by MAES[29] and confirmed by the δ dependence of the VL and the HOMO position as shown later. The increase in the VL was 60 ± 10 meV at the monolayer and much smaller than those in the OVPc-HOPG, ClAlPc-HOPG, and OTiPc-HOPG[20] systems.

For a clearer understanding of the δ dependences of the VL and HOMO band positions, we mapped the intensities of the UPS spectra for the VL and HOMO band regions of each system as a function of δ in Figs. 4–6, which includes the results not shown in Figs. 1–3. In each figure, the horizontal axis represents nominal δ (nm) and the vertical axis represents the electron energy relative to E_F^{sub}. To map the UPS intensities, the background of photoelectrons from the substrate has been subtracted for the HOMO band region. The secondary electron cutoff corresponds to VL, as shown by the white dotted line in the figures. The VL shifts in a staircase pattern in the colored map for $0.36 \leqslant \delta \leqslant 0.7$ nm in Fig. 5. This originates simply from the large step of δ in the deposition steps in δ, and the VL must change gradually, as shown by the white dotted line in Fig. 5. The schematic of the expected molecular orientation at each δ is also superimposed in each figure.[22,23]

Figure 4 clearly shows that the VL of the OVPc-HOPG increases continuously with δ up to $\delta = 0.28$ nm at ~0.3 eV. It then decreases, reaching a constant value similar to that of HOPG at $\delta = 0.66$ nm. From the molecular orientation and the electrostatic potential owing to the permanent dipole of OVPc,[22] these results demonstrate that (i) a monolayer of OVPc is formed at $\delta = 0.28$ nm [point (A) in Fig. 4], (ii) a bilayer formation starts at $\delta \sim 0.28$ nm, and (iii) the bilayer is completed at $\delta = 0.66$ nm [point (B) in Fig. 4], where the dipoles in the first layer are cancelled by those in the second

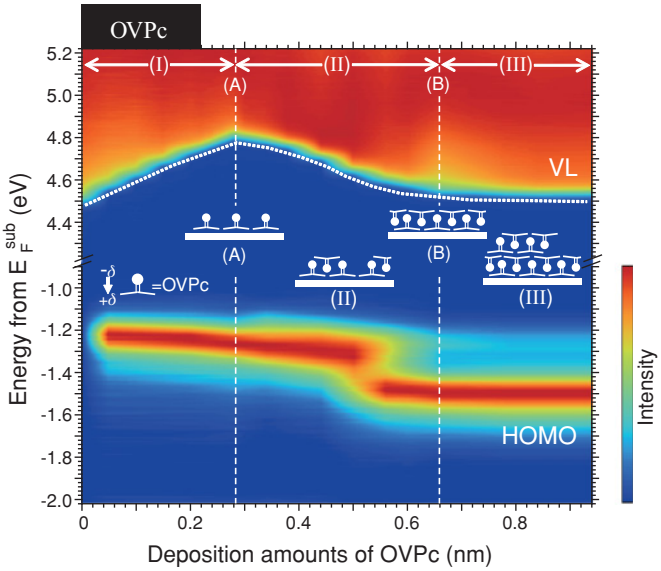

FIG. 4. (Color online) Map of He I UPS spectral intensities for VL and HOMO band regions of the OVPc-HOPG system as a function of deposition amount (δ). The vertical axis represents an electron energy relative to E_F^{sub}. VL corresponds to the cutoff of the secondary electron (indicated by the white dotted line). (I)–(III) indicate regions of monolayer and double-layer formation, and (A) or (B) corresponds to δ of the monolayer and double layer being formed. Schematic of the expected molecular orientation at each deposition amount is also shown.

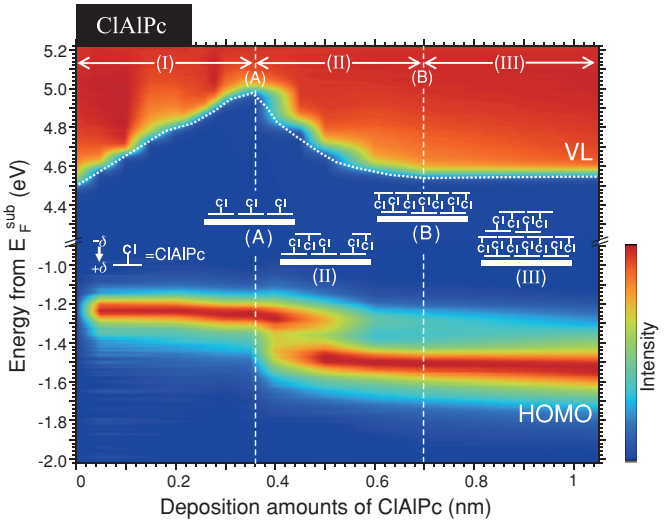

FIG. 5. (Color online) Map of He I UPS spectral intensities for VL and HOMO band regions of the ClAlPc-HOPG system as a function of deposition amount (δ). The vertical axis represents an electron energy relative to E_F^{sub}. VL corresponds to the cutoff of the secondary electron (indicated by the white dotted line). (I)–(III) indicate regions of monolayer and double-layer formation, and (A) or (B) corresponds to δ of the monolayer and double layer being formed. Schematic of the expected molecular orientation at each deposition amount is also shown.

layer. The bilayer formation at $\delta \sim 0.66$ nm can be confirmed by the saturation in the increase in the E_B of the HOMO as well as the change in the HOMO band shape at point B [see also Fig. 1(b)], where the dipole layer potential owing to the oriented monolayer is cancelled by that of the second layer.

For ClAlPc, we see similar results to those for OVPc in Fig. 5, where the VL increases continuously with δ up to $\delta = 0.36$ nm at $\sim$0.47 eV and then decreases, reaching a constant value similar to that of HOPG at $\delta \sim 0.7$ nm. Taking into account the molecular orientation and the electrostatic potential owing to the permanent dipole of ClAlPc,[23] these results can also be understood by considering that (i) the monolayer of ClAlPc is formed at $\delta = 0.36$ nm [point (A) in Fig. 5], (ii) the bilayer formation starts at $\delta = 0.36$ nm, and (iii) the bilayer is completed at $\delta = 0.7$ nm [point (B) in Fig. 5], where the dipoles in the first layer are cancelled by those in the second layer as for OVPc and OTiPc.[20] The bilayer formation can be also confirmed by the E_B position of the HOMO (point B), where the δ dependences of the HOMO band position and shape saturate as seen in Fig. 2(b). As discussed later, however, an interesting increase in the WF exists just before the monolayer formation in both systems.

For CuPc, changes in the VL and the HOMO position saturate at $\delta = 0.37$ nm (indicated by A), although the change in the VL upon the monolayer formation is much smaller than those of the OVPc and ClAlPc systems. This result shows that the monolayer was formed at $\delta = 0.37$ nm, which is consistent with δ for the monolayer formation determined by MAES.[30]

We can obtain the P and α of the monolayers by analyzing the present data on the WF, the energy difference between VL and E_F^{sub}, of each system during monolayer formation within the Topping model. For a semiconductor, a change in WF results from two main contributions:[14] (i) that of the molecular dipole layer ($e\Delta\phi_{Dip}$) and (ii) adsorbate-induced change in surface potential owing to charge exchange through the interface ($e\Delta V_s$). The total WF change ($e\Delta\phi$) is therefore given by

$$e\Delta\phi = e\Delta\phi_{Dip} + e\Delta V_s, \quad (1)$$

In the OVPc and ClAlPc on HOPG systems, we can approximate $e\Delta V_s = 0$ because contribution (ii) is very small

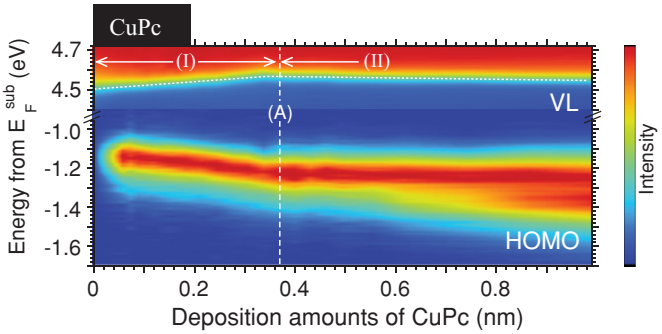

FIG. 6. (Color online) Map of He I UPS spectral intensities for VL and HOMO band regions of the CuPc-HOPG system as a function of deposition amount (δ). The vertical axis represents the electron energy relative to E_F^{sub}. VL corresponds to the cutoff of the secondary electron (indicated by the white dotted line). (I)–(II) indicate regions of monolayer and double-layer formation, and (A) corresponds to δ of the monolayer being formed. At 0.37-nm deposition (A), the VL and HOMO positions show critical changes simultaneously, indicating a monolayer being formed, which was confirmed by MAES Ref. 30.

as understood from the $e\Delta\phi$ observed for the present CuPc-HOPG and in previous studies.[28–30] This can be also supported by the recovery of the VL at the bilayer for OVPc and ClAlPc systems in Figs. 4 and 5 respectively. A small $e\Delta\phi$ in the CuPc-HOPG is related to an induced dipole and/or potential by physisorption and can be included in $e\Delta\phi_{\mathrm{Dip}}$ in the following analyses.

The observed WF change is thus dominated by the density of the oriented dipole of the molecule. In this case, $e\Delta\phi_{\mathrm{Dip}}$ is expressed as[14,17]

$$e\Delta\phi_{\mathrm{Dip}} = \pm\frac{e}{\varepsilon_0}Pn_{\mathrm{Dip}}\left[1+\frac{9\alpha}{4\pi\varepsilon_0}n_{\mathrm{Dip}}^{3/2}\right]^{-1}, \quad f_{\mathrm{dep}} = \frac{9\alpha}{4\pi\varepsilon_0}n_{\mathrm{Dip}}^{3/2}, \tag{2}$$

where n_{Dip} and ε_0 are the dipole density and vacuum permittivity, respectively. The polarizability volume α', which is usually used for condensed media,[31] is defined as

$$\alpha' = \frac{\alpha}{4\pi\varepsilon_0}. \tag{3}$$

In passing, one should be careful about the reported value of the polarizability, because $4\pi\alpha$ is often used as the value of the polarizability in the surface science field.[17,19] The dipole density may be expressed as[18]

$$n_{\mathrm{Dip}} = \frac{\theta}{d^2}b, \tag{4}$$

where θ is the coverage of OVPc, ClAlPc, and CuPc ($0 \leqslant \theta \leqslant 1$ ML), d is the lattice constant of each monolayer system, and b is a constant related to the lattice structure of adsorbed molecules ($b=1$ for a square lattice and $2/\sqrt{3}$ for a triangle one). The second term in parentheses in Eq. (2), called the depolarization factor f_{dep}, is a correction to the WF change owing to an interaction between the dipoles.[1,14,17] This contribution reduces the effective electric field at the site of a particular dipole. As the unit cell of the phthalocyanine monolayer on graphite was reported to be square for both CuPc ($a_1 = 1.50$ nm, $b_1 = 1.50$ nm at 77 K)[32,33] and square for ClAlPc ($a_2 = 1.51$ nm, $b_2 = 1.51$ nm nm at 77 K)[27] from STM studies, b is 1.[18] Hence, Eq. (2) becomes

$$e\Delta\phi_{\mathrm{Dip}} = \pm\frac{eP\theta}{\varepsilon_0 d^2}\left[1+9\alpha'\left(\frac{\theta}{d^2}\right)^{3/2}\right]^{-1}, \tag{5}$$

where we use the polarizability volume α'. Here, we assume that the lattice constant of the OVPc monolayer is the same as that of the ClAlPc-HOPG system; thus, $d=1.51$ nm for both OVPc and ClAlPc. We also reanalyze the previous OTiPc data[20] with $d=1.51$ nm.

Figures 7(a)–7(d) show the WF versus molecular coverage (θ) plot and some fitting curves, as well as the previous results on the OTiPc-HOPG system.[20] In these plots $\theta = 1$ corresponds to the monolayer, which was identified by the vacuum level change, HOMO band structure in UPS, and spectral intensity of MAES, and the θ scale is assumed to be proportional to δ for $0 < \theta < 1$. Therefore, the θ dependence of the WF deviates suddenly from that expected from Eq. (5) when the intermolecular distance is changed more rapidly than that expected from the variation of δ or θ. For ClAlPc in Fig. 7(a), we clearly observed a steplike increase in the WF

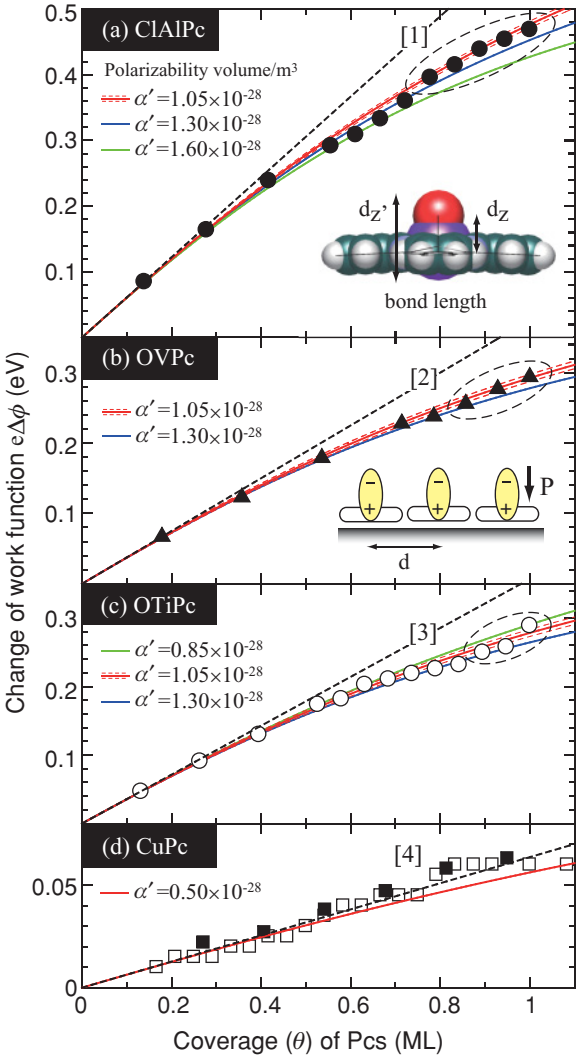

FIG. 7. (Color online) Coverage dependence of the work function for (a) ClAlPc, (b) OVPc, (c) OTiPc Ref. 20, and (d) CuPc, where 1 ML ($\theta=1$) corresponds to $\delta=0.36$, 0.28, 0.38 Ref. 20, and 0.37 nm, respectively. In (d), results of independent experiments (■) are superimposed to show experimental accuracy. In the low-coverage region, WF increases linearly along dashed lines [1], [2], [3], and [4], giving a dipole moment of 3.70 D for ClAlPc, 2.27 D for OVPc, 2.16 D for OTiPc, and 0.38 D for CuPc. The colored curves in each panel represent fitting curves with different α' (see text). The colored curve coupled with two dashed curves in (a), (b), and (c) gives the most plausible α'. The separation of these two dashed curves corresponds to an error coming from the determination of the dipole moment. The definition of the bond length of the central part (d_z) and the effective thickness including electron spread (d_z') are shown in (a) (see text and Table I). A schematic representation of the molecular orientation and the direction of the dipole (P) of all dipole phtalocyanines is shown in (b).

near $\theta \sim 0.72$. Note here that such a sudden increase in the WF in ClAlPc can be seen also in OVPc at $\theta \sim 0.85$, as marked by the dashed ovals in Figs. 7(a) and 7(b). Such a discontinuity in the coverage dependence also exists for OTiPc, which was not mentioned in the previous paper.[20] The discontinuity was observed for the three dipole systems and not for nondipole

CuPc as shown in Fig. 7(d), where the CuPc system shows a smooth increase in the WF with θ. It is easily expected from Eq. (2) that the discontinuity in the coverage dependence of the WF near $\theta \sim 1$ for the three dipole molecules can be related to a rapid increase in the dipole density.

As the physical structure of a molecular ultrathin film is governed by a fine balance between weak molecule-molecule interactions and a laterally varying weak molecule-substrate interaction potential, the discontinuities may originate from a structure transition mediated by the balance of the repulsive intermolecular dipole-dipole interaction and the attractive dispersion interaction. Kroeger *et al.* reported that spot profile analysis–low-energy electron diffraction (SPA-LEED) of a CuPc-Ag(111) system has a rich structure phase with two-dimensional-gaslike disordered and ordered structures for the CuPc.[34] In particular, they showed a continuous change in lattice parameters with increasing coverage for long-range-ordered structures just below monolayer (ML) coverage (0.89–1 ML at 300 K and 0.75–1 ML at 130 K) owing to a substrate-mediated repulsive intermolecular interaction similar to the case of tin-phthalocyanine–Ag(111).[35] On the other hand, Mannsfeld and Fritz showed that the point-on-line coincidence reduces the interface potential energy, where all overlayer molecules lie on primitive lattice lines of the substrate surface lattice.[36,37] As the physical structure of organic ultrathin films on graphite is governed by a fine balance between various molecule-molecule interactions and a laterally varying weak molecule-substrate interaction, the packing geometry of molecules may change suddenly during monolayer formation in the present case. This is because the dipole-dipole repulsive interaction ($\sim r^{-3}$, where r is the intermolecular distance) is a longer-range one than other intermolecular attractive interactions (e.g., the dispersion interaction $\sim r^{-6}$),[38] and the molecules prefer to lie on primitive lattice lines of the graphite surface.[36] Accordingly, this effect may result in a sudden increase in the θ dependence of the WF near $\theta = 1$ owing to a faster increase in the dipole density than that extrapolated from a lower-θ region, and this increase may be larger for phthalocyanine with a larger dipole moment. The values of the dipole moment are in the order of P (ClAlPc) > P (OVPc) > P (OTiPc) $\gg$ P (CuPc) as determined below, and the discontinuity is larger for the larger-dipole molecule. These results are consistent with the above consideration. From these results, the discontinuity can be ascribed to a structure transition that is related to the dipole-dipole repulsive interaction.

Prior to analyzing the higher-θ region, we first obtain P by analyzing the θ dependence of WF in the low-θ region. For the low-θ region, we obtain the following relation because $f_{\mathrm{dep}} \ll 1$:

$$e\Delta\phi = \pm\frac{e}{\varepsilon_0}P\frac{\theta}{d^2} = \pm\frac{e}{\varepsilon_0}Pn_{\mathrm{Dip}}. \tag{6}$$

In this case, WF increases linearly with n_{Dip} and thus P is determined by the slope of the $e\Delta\phi$-vs-θ plot. In the low-θ region, we see that WF changes nearly linearly with θ, as shown by dashed lines [1]–[4] in Figs. 7(a)–7(d), respectively. We thus obtained P as 3.70 Debye (D) for ClAlPc, 2.27 D for OVPc, 2.16 D for OTiPc, and 0.38 D for CuPc. The experimental P and calculated P of each molecule, which are shown in Table I, were different. The calculated P was obtained using the DFT method with the standard B3LYP/LANL2DZ in the optimized structure of each molecule. The experimental value was smaller than the calculated value for all dipole molecules. We examined other calculations for P and found that the calculated value is very sensitive to the distance between the central metal and the protruding atom. We speculate that the difference between the experimental and calculated P values originates mainly from the accuracy in the calculated chemical structure, because the difference between the experimental and calculated P values is larger than the induced dipole by a weak molecule-graphite interaction that was observed for the CuPc-HOPG.

Using the obtained P value, we can estimate α' by fitting Eq. (5) with the WF change in the higher-θ region by setting α' as a variable parameter. However, there is a sudden increase in the WF change in the higher-θ region depending on the molecular dipole. In this case, Eq. (5) implies that the WF change becomes larger owing to the rapid increase in the dipole density near $\theta = 1$. Thus we must use the data above the θ value, at which the discontinuity appears, to determine the α' in the monolayer. Given these considerations, we fitted Eq. (5) with the observed results (the colored curve in each figure) and, using the lattice parameter determined for the ClAlPc Ref. 27 and CuPc Ref. 32 monolayers, obtained $\alpha' = 1.05 \times 10^{-28}$ m^3 for ClAlPc and OVPc, and $\alpha' < 0.50 \times 10^{-28}$ m^3 for CuPc. For OTiPc, $\alpha' = 1.05 \times 10^{-28}$ m^3 or 0.85×10^{-28} m^3, where the latter value was from the uppermost fitting curve in Fig. 7(c). The reevaluated value for OTiPc was slightly smaller than the previously determined value.[20] The results are summarized in Table I.

We next estimate the dielectric constants of all polar phthalocyanine monolayer systems (OTi-, OV-, ClAl-Pc) using the following two methods. (i) First, the Helmholtz equation,[10]

$$\Delta V = \frac{\mu\cos\varphi}{\varepsilon^H\varepsilon_0}, \tag{7}$$

is used, where ΔV is the surface-potential change and corresponds to $\Delta\phi$, μ is the dipole moment per unit area, φ is the angle between the dipole and the surface normal, and ε^H is the dielectric constant in the Helmholtz model. In Eq. (7), the number density of dipoles is assumed to be 1 per 1.51×1.51 nm^2 Ref. 27. Using the obtained P and observed WF change, we determined the dielectric constant in all systems as summarized in Table I, where the comparison of the estimated P and calculated P is also summarized. (ii) Second, the relation between ε and α' is applied, which is expressed as[39]

$$\varepsilon = 1 + \chi_e, \quad \chi_e = \frac{N}{V}\alpha'. \tag{8}$$

Here, χ_e is the electric susceptibility, and N/V is the number of molecules per unit volume. In Eq. (8), we obtained N/V from molecular thickness and the area for the molecule. For the molecular thickness, we used two different thicknesses: the first was the interatomic distance at the dipole (d_z), and the second was an effective molecular thickness that includes the electron spread obtained by adding the ion radius of each atom to d_z (d_z'). d_z is assumed to be the calculated value from the optimized molecular structure in the DFT calculation. The

TABLE I. Dielectric properties of the monolayer of polar phthalocyanines and Cu-phthalocyanine on graphite. $\Delta e\phi$, P, α', and ε are the work-function change (vacuum level shift), electric dipole moment, polarizability volume, and dielectric constant, respectively. The structure parameters used to estimate α' are summarized.

	ClAlPc	OVPc	OTiPc[a]	CuPc
$\Delta e\phi$ (eV)	0.47 ± 0.01	0.30 ± 0.01	0.29 ± 0.01	0.06 ± 0.01
P (D)	3.70 ± 0.04	2.27 ± 0.04	2.16 ± 0.04	0.38 ± 0.04
Calc. P (D)[b]	5.28	2.79	3.73	0
α' (m^3)[c]	1.05×10^{-28}	1.05×10^{-28}	1.05×10^{-28}(0.85×10^{-28})[d]	$<0.50 \times 10^{-28}$
ε^{H}[e]	1.30 ± 0.04	1.25 ± 0.06	1.23 ± 0.06	<1.11 ± 0.03
ε^{d_z}[f]	1.20	1.28	1.28(1.22)[l]	–
$\varepsilon^{d'_z}$[g]	1.03	1.13	1.12(1.10)[l]	<1.06
d_z (nm)[h]	0.228	0.160	0.164	–
d'_z (nm)[i]	0.448	0.362	0.389	0.37[j]
Square unit cell	1.51×1.51 nm^2[k]	ClAlPc cell assumed	ClAlPc cell assumed	1.50×1.50 nm^2[k]

[a]Reevaluated values using lattice parameters of $a, b = 1.51$ nm (see Ref. 20). α' value in Ref. 20 is $4\pi\alpha'$.
[b]Dipole of free molecule obtained by DFT calculation (B3LYP/LANL2DZ).
[c]Polarizability volume of single molecule in monolayer $\alpha' = \alpha/4\pi\varepsilon_0$.
[d]Value in parentheses is the expected smallest value [see the uppermost fitting curve in Fig. 7(c)].
[e]ε estimated by the Helmholtz equation [Eq. (7)].
[f]ε estimated by Eq. (8), where the molecular thickness is assumed to be d_z.
[g]ε estimated by Eq. (8), where the molecular thickness is assumed to be d'_z.
[h]Bond length of O-Ti, O-V, and Cl-Al obtained by DFT calculation (B3LYP/LANL2DZ).
[i]Effective thickness of the molecular layer with electron spread obtained by adding an ion radius of each atom to d_z.
[j]Nominal thickness of the monolayer determined by MAES experiments Ref. 30.
[k]Values are from Ref. 27 (ClAlPc) and Ref. 32 (CuPc).
[l]Values in parentheses were obtained with $\alpha' = 0.85 \times 10^{-28}$ [m^3].

schematic representations of d_z and d'_z are shown in the inset in Fig. 7(a). ε^{d_z} and $\varepsilon^{d'_z}$ are obtained by assuming the molecular thicknesses to be d_z and d'_z, respectively. All these values and those for CuPc are summarized in Table I.

Finally, we compare the estimated values of ε obtained by using methods (i) and (ii). The fact that the ε values estimated by using the two different methods were almost the same clearly demonstrates that the Helmholtz equation is applicable to a system that is not a continuum medium and to a system with a dipole-dipole interaction if the value of the dipole in the Helmholtz equation involves the depolarization effect. The ε estimated for the present molecular sheet of large molecules is much smaller than those of other organic dipole layer systems such as SAMs because the dipole density in the present system is smaller owing to the larger molecular size.[10]

IV. CONCLUSION

We achieved the monolayer formation of polar phthalocyanines (ClAlPc, OVPc, and OTiPc) and nonpolar CuPc on an inert graphite surface and measured the coverage dependence of WF for these molecules. By analyzing the WF change using the Topping model, we obtained the electric dipole moment and polarizability of the phthalocyanines in the monolayer. We also estimated the dielectric constant of the phthalocyanine monolayers and found that the values estimated using the macroscopic Helmholtz equation and the nanoscopic Topping model were almost the same. This demonstrates that the Helmholtz equation is applicable to the nanoscale system, although the nanoscale system is not a continuum medium. Furthermore, we observed an effect of the dipole-dipole repulsive interaction on the intermolecular two-dimensional structure, which plays an important role in monolayer growth and structure in weakly interacting polar-molecule–substrate systems.

ACKNOWLEDGMENTS

This work was partly supported by a Grant-in-Aid for Scientific Research (A), a Grant-in-Aid for Young Scientists (A), and global COE programs (G03 by MEXT).

*Present address: NHK Science and Technology Research Laboratories, 1-10-11 Kinuta, Setagaya-Ku, Tokyo 157-8510, Japan.
†Corresponding author: kera@faculty.chiba-u.jp

[1]A. Natan, L. Kronik, H. Haick, and R. T. Tung, Adv. Mater. (Weinheim, Ger.) **19**, 4103 (2007).
[2]J. Hwang, A. Wan, and A. Kahn, Mater. Sci. Eng., R **64**, 1 (2009).
[3]Y. Gao, Mater. Sci. Eng., R **68**, 39 (2010).
[4]I. H. Campbell, S. Rubin, T. A. Zawodzinski, J. D. Kress, R. L. Martin, D. L. Smith, N. N. Barashkov, and J. P. Ferraris, Phys. Rev. B **54**, 14321 (1996).
[5]I. H. Campbell, J. D. Kress, R. L. Martin, D. L. Smith, N. N. Barashkov, and J. P. Ferraris, Appl. Phys. Lett. **71**, 3528 (1997).

[6]L. Zuppiroli, L. Si-Ahmed, K. Kamaras, F. Nüesch, M. N. Bussac, D. Ades, A. Siove, E. Moons, and M. Grätzel, Eur. Phys. J. B **11**, 505 (1999).
[7]A. Vilan, A. Shanzer, and D. Cahen, Nature (London) **404**, 166 (2000).
[8]C. Ganzorig, K.-J. Kwak, K. Yagi, and M. Fujihira, Appl. Phys. Lett. **79**, 272 (2001).
[9]G. Ashkenasy, D. Cahen, R. Cohen, A. Shanzer, and A. Vilian, Acc. Chem. Res. **35**, 121 (2002).
[10]M. Bruening, R. Cohen, J. F. Guillemoles, T. Moav, J. Libman, A. Shanzer, and D. Cahen, J. Am. Chem. Soc. **119**, 5720 (1997).
[11]S. D. Evans, E. Urankar, A. Ulman, and N. Ferris, J. Am. Chem. Soc. **113**, 4121 (1991).
[12]J. Topping, Proc. R. Soc. London Ser. A **114**, 67 (1927).
[13]J. R. MacDonald and C. A. Barlow, J. Chem. Phys. **39**, 412 (1963).
[14]H. Lüth, *Surface and Interfaces of Solid Materials* (Springer, Berlin, 1995), p. 509.
[15]D. M. Taylor and G. F. Bayes, Phys. Rev. E **49**, 1439 (1994).
[16]R. W. Verhoef and M. Asscher, Surf. Sci. **391**, 11 (1997).
[17]G. Gensterblum, K. Hevesi, B. Y. Han, L. M. Yu, J. J. Pireaux, P. A. Thiry, R. Caudano, A. A. Lucas, D. Bernaerts, S. Amelinckx, G. Van Tendeloo, G. Bendele, T. Buslaps, R. L. Johnson, M. Foss, R. Feidenhans'l, and G. Le Lay, Phys. Rev. B **50**, 11981 (1994).
[18]M. Pivetta, F. Patthey, W. D. Schneider, and B. Delley, Phys. Rev. B **65**, 045417 (2002), and references therein.
[19]S. Kera, Y. Yabuuchi, H. Yamane, H. Setoyama, K. K. Okudaira, A. Kahn, and N. Ueno, Phys. Rev. B **70**, 085304 (2004).
[20]H. Fukagawa, H. Yamane, S. Kera, K. K. Okudaira, and N. Ueno, Phys. Rev. B **73**, 041302(R) (2006).
[21]A. Natan, Y. Zidon, Y. Shapira, and L. Kronik, Phys. Rev. B **73**, 193310 (2006).
[22]H. Fukagawa, H. Yamane, S. Kera, K. K. Okudaira, and N. Ueno, J. Electron Spectrosc. Relat. Phenom. **144-147**, 475 (2005).
[23]S. Kera, H. Yamane, H. Honda, H. Fukagawa, K. K. Okudaira, and N. Ueno, Surf. Sci. **566-568**, 571 (2004).
[24]H. Yamane, H. Fukagawa, S. Nagamatsu, M. Ono, S. Kera, K. K. Okudaira, and N. Ueno, IPAP Conf. Series **6**, 19 (2005), [http://www.ipap.jp/ipap_cs.html].
[25]S. Kera, K. K. Okudaira, Y. Harada, and N. Ueno, Jpn. J. Appl. Phys. **40**, 783 (2001).
[26]S. Kera, A. Abduaini, M. Aoki, K. K. Okudaira, N. Ueno, Y. Harada, Y. Shirota, and T. Tsuzuki, Thin Solid Films **327-329**, 278 (1998).
[27]Y. L. Huang, W. Chen, R. Wang, T. C. Niu, S. Kera, N. Ueno, J. Pflaum, and A. T. S. Wee, Chem. Commun. **46**, 9040 (2010).
[28]S. Kera, H. Yamane, I. Sakuragi, K. K. Okudaira, and N. Ueno, Chem. Phys. Lett. **364**, 93 (2002).
[29]S. Kera, H. Yamane, and N. Ueno, Prog. Surf. Sci. **84**, 135 (2009).
[30]H. Yamane, Y. Yabuuchi, H. Fukagawa, S. Kera, K. K. Okudaira, and N. Ueno, J. Appl. Phys. **99**, 093705 (2006).
[31]N. Sato, K. Seki, and H. Inokuchi, J. Chem. Soc. Faraday Trans. II **77**, 1621 (1981).
[32]Y. L. Huang, H. Li, J. Ma, H. Huang, W. Chen, and A. T. S. Wee, Langmuir **26**, 3329 (2010).
[33]We use the newest STM result on a CuPc-HOPG Ref. 32 in the present analyses, while in our previous paper Ref. 20 we used the CuPc unit-cell parameters ($a = 1.37$ nm, $b = 1.36$ nm, $\angle ab = 90.3^\circ$, temperature unknown) reported in the following paper: C. Ludwig, R. Strohmaier, J. Petersen, B. Gompf, and W. Eisenmenger, J. Vac. Sci. Technol. B **12**, 1963 (1994).
[34]I. Kroeger, B. Stadtmüller, C. Stadler, J. Ziroff, M. Kochler, A. Stahl, F. Pollinger, T.-L. Lee, J. Zegenhagen, F. Reinert, and C. Kump, New J. Phys. **12**, 083038 (2010).
[35]Ch. Stadler, S. Hansen, I. Kroeger, C. Kumpf, and E. Umbach. Nat. Phys. **5**, 153 (2009).
[36]S. C. B. Mannsfeld and T. Fritz, Phys. Rev. B **69**, 075416 (2004).
[37]S. C. B. Mannsfeld and T. Fritz, Phys. Rev. B **71**, 235405 (2005).
[38]See, for example, P. W. Atkins, *Physical Chemistry* (Oxford University Press, London, 1998), Chap. 22.
[39]J. C. Slater and N. H. Frank, *Electromagnetism* (McGraw-Hill, New York, 1947), Chap. 4.